

# Automation of NLO processes and decays and POWHEG matching in WHIZARD

Jürgen Reuter<sup>1</sup>, Bijan Chokoufé<sup>1</sup>, André Hoang<sup>2,3</sup>, Wolfgang Kilian<sup>4</sup>, Maximilian Stahlhofen<sup>5,1</sup>, Thomas Teubner<sup>6</sup>, Christian Weiss<sup>1,4</sup>

<sup>1</sup> DESY Theory Group, Notkestr. 85, 22607 Hamburg, Germany

<sup>2</sup> University of Vienna, Faculty of Physics, Boltzmannngasse 5, 1090 Vienna, Austria

<sup>3</sup> Erwin Schrödinger International Institute for Mathematical Physics, University of Vienna, Boltzmannngasse 9, 1090 Vienna, Austria

<sup>4</sup> University of Siegen, Emmy-Noether Campus, Walter-Flex-Str. 3, 57068 Siegen, Germany

<sup>5</sup> PRISMA Cluster of Excellence, Institute of Physics, Johannes Gutenberg University, 55128 Mainz, Germany

<sup>6</sup> University of Liverpool, Department of Mathematical Sciences, Liverpool L69 3BX, U.K.

E-mail: [juergen.reuter@desy.de](mailto:juergen.reuter@desy.de), [bijan.chokoufe@desy.de](mailto:bijan.chokoufe@desy.de), [andre.hoang@univie.ac.at](mailto:andre.hoang@univie.ac.at), [kilian@physik.uni-siegen.de](mailto:kilian@physik.uni-siegen.de), [mastahlh@uni-mainz.de](mailto:mastahlh@uni-mainz.de), [thomas.teubner@liverpool.ac.uk](mailto:thomas.teubner@liverpool.ac.uk), [christian.weiss@desy.de](mailto:christian.weiss@desy.de)

**Abstract.** We give a status report on the automation of next-to-leading order processes within the Monte Carlo event generator WHIZARD, using GoSam and OpenLoops as provider for one-loop matrix elements. To deal with divergences, WHIZARD uses automated FKS subtraction, and the phase space for singular regions is generated automatically. NLO examples for both scattering and decay processes with a focus on  $e^+e^-$  processes are shown. Also, first NLO-studies of observables for collisions of polarized leptons beams, e.g. at the ILC, will be presented. Furthermore, the automatic matching of the fixed-order NLO amplitudes with emissions from the parton shower within the POWHEG formalism inside WHIZARD will be discussed. We also present results for top pairs at threshold in lepton collisions, including matching between a resummed threshold calculation and fixed-order NLO. This allows the investigation of more exclusive differential observables.

## 1. The WHIZARD Event Generator

WHIZARD [1] is a multi-purpose event generator for in principle arbitrary processes at hadron and lepton colliders. Being able to treat beam-spectra and initial-state photon radiation, it is especially suited for lepton collider physics studies. Moreover, its built-in scripting language SINDARIN allows for the analysis in the same framework. WHIZARD is written in Fortran2003. Its structure is strictly object-oriented, so that a modular setup enables the convenient interface to numerous other programs. The main sub-components of WHIZARD are O'Mega [2], VAMP [3] and CIRCE [4]: O'Mega provides multi-leg tree-level matrix elements using the helicity formalism. VAMP is used for Monte-Carlo integration and grid sampling. CIRCE creates and evaluates lepton beam spectra. Color factors are evaluated using the color-flow formalism [5]. WHIZARD can be used for event generation on parton level as well as for the subsequent shower simulation. For this purpose, it has its own analytical and  $k_T$ -ordered parton shower [6] as well as a built-in interface to Pythia6 [7]. An automated interface to Pythia8 [8] or HERWIG++ [9] is not yet present, but planned. Though WHIZARD spearheaded many BSM phenomenological studies [10–16], these proceedings focus on the automation of SM QCD NLO corrections and non-relativistic top threshold resummation.

## 2. Automated NLO Calculations in WHIZARD

Next-to-leading order (NLO) calculations have become standard for the prediction of most observables during the last decade. Substantial progress has been made in the automation of loop matrix-element computations as well as in NLO parton shower matching [17, 18]. At the LHC, NLO simulations are routinely employed. Computer programs in this field cover a range from dedicated, single-purpose codes to automated multi-purpose event generators.

With the ILC approaching its possible approval phase, ILC studies become more specific [19], thereby increasing the need for easy to use NLO programs. Here, we want to combine the expertise of WHIZARD in the field of lepton collisions with the improved accuracy of NLO predictions. There have been earlier works on NLO QED extensions to WHIZARD for certain supersymmetric processes [20, 21] as well as on NLO QCD corrections for  $pp \rightarrow b\bar{b}b\bar{b}$  [22, 23] using Catani-Seymour subtraction. However, the fully generic NLO framework is a recent development.

Automated NLO programs deal with the infrared divergences of real and virtual matrix elements by using subtraction procedures. These rely on the extraction of the soft and collinear limit in its most generic form. This is possible because the  $\mathcal{O}(\alpha_s)$ -corrections factorize in the corresponding limits. These subtraction terms  $d\sigma^S$  are then added and subtracted, such that

$$d\sigma^{\text{NLO}} = d\sigma^{\text{LO}} + \underbrace{\int_{n+1} (d\sigma^{\text{R}} - d\sigma^{\text{S}})}_{\text{finite}} + \underbrace{\int_{n+1} d\sigma^{\text{S}} + \int_n d\sigma^{\text{V}}}_{\text{finite}}. \quad (1)$$

The explicit form of  $d\sigma^S$  is arbitrary. The two most common schemes employed are Catani-Seymour subtraction [24] and the FKS (Frixione-Kunszt-Signer) scheme [25]. WHIZARD uses the latter. The program automatically finds the singular regions involved in the desired process and computes the subtraction terms to the real matrix element correspondingly.

NLO computations require virtual loop matrix elements. However, `0'Mega` can only generate tree-level matrix elements. So, to obtain virtual matrix elements, external programs, so-called One-Loop Providers (OLP), can be interfaced to WHIZARD. Up to now, there are working interfaces to `GoSam` [26] and `OpenLoops` [27]. They use the Binoth Les Houches Accord (BLHA) [28], which unifies the interface between Monte-Carlo generator and OLPs. The BLHA interface in WHIZARD is generic, meaning that every other matrix element generator which complies to the BLHA standard can be interfaced very easily in the same fashion.

The NLO functionality of WHIZARD has first been presented in [29], where we have focussed our discussion on fixed-order off-shell top production. In the following, we want to present the newest developments in WHIZARD for NLO.

### 2.1. Treatment of Resonances

A recent development in WHIZARD is the special treatment of radiative corrections occurring from particles which originate from a common resonance. This issue has been extensively discussed in [30]. We have automated the scheme discussed therein in WHIZARD.

Subtraction methods like FKS lose accuracy when after the construction of the real phase space, the resonance momentum deviates significantly from its value in the Born phase space. This affects the propagator both in the real and the Born matrix element, which is part of the subtraction terms. The real matrix element and its approximation therefore do not match perfectly, impairing the convergence of the integration and distorting the invariant mass spectrum in event generation [30].

This problem is solved by employing a phase space mapping that generates the real phase space in such a way that the resonance momentum is conserved. Thus the real matrix element is evaluated at the same point on the resonance's Breit-Wigner curve. However, this

**Table 1.** Comparison of integration histories for the standard and resonance-aware subtraction at  $\sqrt{s} = 800$  GeV. The Coulomb singularity which arises from  $\gamma \rightarrow \mu^+ \mu^-$  has been cut out by imposing  $m_{\mu\mu} > 20$  GeV. Each iteration uses 12000 calls.

$n_{it}$	$\sigma[fb]$ , standard	Error[%]	$\sigma[fb]$ , resonances	Error[%]
1	9.68118	66.30	2.90570	2.87
2	2.85397	8.25	2.85920	1.82
3	2.49076	26.25	2.92779	1.40
4	2.76956	34.91	2.85123	1.40
5	2.43462	19.80	2.88554	1.34
5	2.75391	7.15	2.88420	0.71

**Table 2.** Real-subtracted integration component and, in the case of resonance-aware subtraction, soft mismatch, for  $\Gamma_H = 1000$  GeV at  $\sqrt{s} = 800$  GeV.

Method	$\sigma_{\text{soft}}[fb]$	$\sigma_{\text{mism}}[fb]$	$n_{\text{calls}}$
standard	$-3.31997 \pm 0.62\%$	0	$5 \times 100000$
resonances	$-1.62098 \pm 0.29\%$	$-1.70388 \pm 0.56\%$	$5 \times 20000$ (soft) + $5 \times 20000$ (mismatch)

approach comes with the drawback of increased complexity in the implementation, since now the calculation has to be aware of the additional singular regions belonging to different resonance histories. Moreover, the so-called soft mismatch (Eq. (3.59) in [30]) enters the calculation as an additional new component of the integration. This is due to the fact that the sum over all singular regions does not reproduce the full real matrix element in this approach, because for each singular region, the FKS mapping is evaluated in the associated resonance’s frame of reference. However, usual FKS requires all subtraction terms to be evaluated in the same frame of reference. This property can be restored, yielding the soft mismatch term.

The implementation of the resonance-aware subtraction has been applied to the process  $e^+ e^- \rightarrow b\bar{b}\mu^+\mu^-$ , where there is one resonance topology with two associated resonance histories, namely  $Z/H \rightarrow b\bar{b}$ . This process is also of interest in studies of Higgsstrahlung processes at lepton colliders. We have set  $m_b = 4.2$  GeV, so that collinear divergences do not occur. Without resonance mappings, we observe that the integration does not perform well, due to the very narrow Higgs resonance ( $\Gamma_H \sim 4$  MeV). Even a relatively soft gluon emission is enough to alter the resonance momentum in such a way that the soft approximation does not fit well enough with the real matrix element. Using the resonance-aware subtraction we obtain significantly better results, as can be clearly seen in Table 1. Taking the large-width limit yields a good integration also for the non-resonant case, as desired. Table 2 shows that both calculations give the same result in this limit. However, the non-resonant approach needs significantly more integration calls to reach the same accuracy as its resonance-aware counterpart. Figure 1 shows a scan of the total cross section. The generation of fixed-order NLO events has been modified for the use with resonance-aware subtraction. In the earlier version of WHIZARD, weighted  $N$ -particle events were produced with weight  $\mathcal{B} + \mathcal{V} + \mathcal{S}$  and associated with  $N + 1$ -particle events with weight  $\mathcal{R}_{\alpha_r}$  for each singular region  $\alpha_r$ . The events are saved in HepMC-files. If resonances are included,

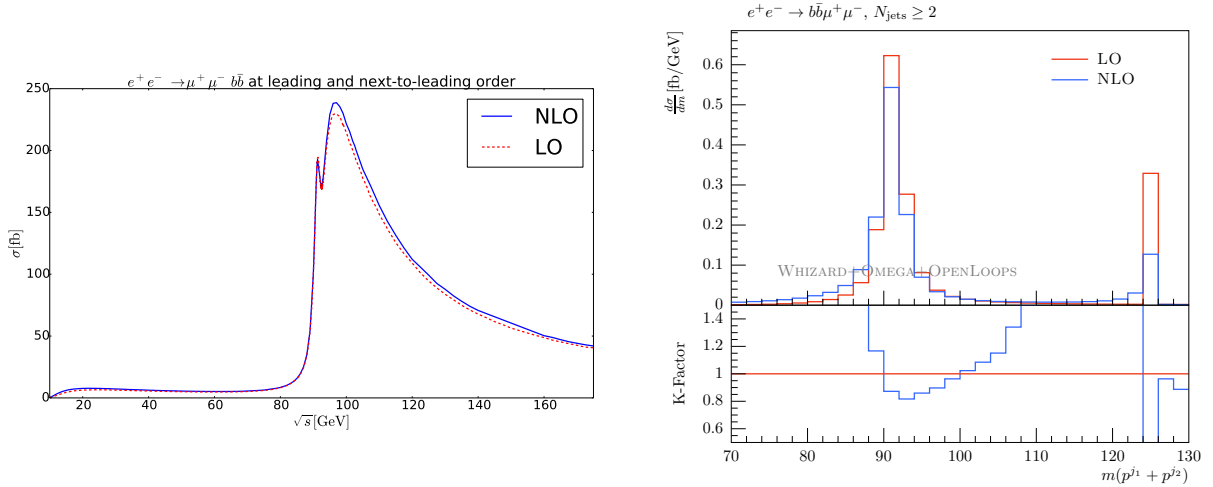


**Figure 1.** Left:  $\sigma_{\text{tot}}$  at the  $Z\mu\mu$  and  $Zbb$  resonance. Right: Invariant mass distribution of the two hardest jets at  $\sqrt{s} = 800$  GeV. Jets have been clustered using **FastJet** [31]. The  $Z$  and especially the  $H$  peak are being washed out by gluon emissions.

different  $\alpha_r$  can yield the same phase space if they only differ by the underlying resonance mass. Therefore, to save disk space, the number of real events now is the number of different possible phase spaces. Their weight is the sum of all  $\mathcal{R}_{\alpha_r}$  whose  $\alpha_r$  belong to the same phase space. Figure 1 shows an example of NLO event generation in **WHIZARD**.

## 2.2. Other features

**WHIZARD** is able to produce events according to the POWHEG scheme, which can be used as input to parton showers and preserve the NLO accuracy of the subsequent simulations. This has been discussed in [32] and will not be elaborated further here.

Apart from the major NLO functionalities above, **WHIZARD** also can now deal with several minor aspects of NLO calculations. First, **WHIZARD** can also compute decay widths at next-to-leading order and generate fixed-order events accordingly. The first use case here is the top decay  $t \rightarrow bW$ . The computation takes into account both the initial-state gluon emissions from the top quark and final-state emissions from the bottom quark. The results of this computation play a crucial role in the study of the top threshold described in the next section, where it is important to keep consistency between the input parameters and the top width used.

Second, NLO calculations can be performed using polarized lepton beams. This is a desirable feature for future studies at the ILC or CLIC, which will operate with polarized leptons. For this purpose, **WHIZARD** uses a modified BLHA interface to **OpenLoops**, which allows it to provide the virtual matrix elements individually for each helicity configuration of the colliding lepton pair.

## 3. Top Threshold Resummation and Matching to the Continuum

High-energy lepton colliders operating at the top threshold or close to it allow for the most precise method to measure the mass of the top quark known to date. However, at threshold the top quark pair is non-relativistic and can thus form a toponium quasi-bound state, due to the attractive top quark potential. This potential relies on the exchange of an arbitrary number of virtual gluons between the tops. The bound-state effects give rise to Coulomb singularities  $(\alpha_s/v)^n$  and large logarithms  $\ln^n v$  in the perturbative expansion of the cross section. Here,  $v \sim \alpha_s \sim 0.1$  is the relative velocity of the non-relativistic top quarks. The resummation of the

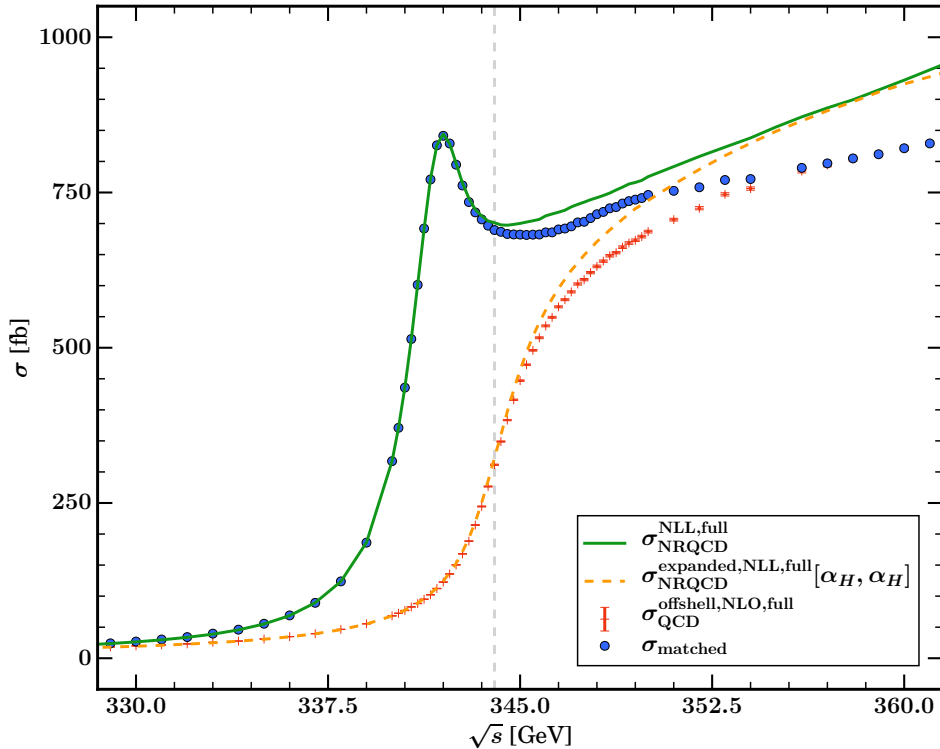


**Figure 2.** Matching the NLL resummed threshold prediction to the fixed-order NLO QCD continuum for the total cross section of the process  $e^+e^- \rightarrow W^+bW^-$ . The blue dots show the result obtained by the (preliminary) matching prescription between vNRQCD and the continuum. The solid green line corresponds to the insertion of the NLL form factor from TOPPIK into the Born process. The dashed orange curve shows the same result with the form factor expanded to first order in  $\alpha_s$ . The red crosses represent the full relativistic fixed-order NLO result.

threshold enhanced terms can be carried out in the vNRQCD framework [33–37]. The R-ratio then takes the schematic form [38]

$$R = \frac{\sigma_{t\bar{t}}}{\sigma_{\mu\mu}} = v \sum_k \left(\frac{\alpha_s}{v}\right)^k \sum_l (\alpha_s \ln v)^l \times \underbrace{\left\{ 1(LL); \alpha_s, v(NLL); \alpha_s^2, \alpha_s v, v^2(NNLL); \dots \right\}}_{\text{effective } t\bar{t}V \text{ vertex}}. \quad (2)$$

In WHIZARD, the resummation is achieved by replacing the  $t\bar{t}\gamma$  and  $t\bar{t}Z$  vertices by non-relativistic form factors at NLL accuracy using the external code TOPPIK [39]. This interface was first discussed in [40]. A recent development is the matching of the vNRQCD-approximation to the relativistic continuum, complementing the accuracy of the two approximations. The matching between the resummed prediction at threshold and the relativistic NLO result, which is the reliable result for  $\sqrt{s} \gg 2m_t$ , is based on two main concepts. First, we have to subtract the first order expansion of the resummed computation when we want to add the NLO contributions. This has to be done in a way that respects the relevant scales of the vNRQCD calculation (hard  $m_t$ , soft  $m_tv$  and ultra-soft  $m_tv^2$ ). In Figure 2 we can see how this expansion evaluated at the hard scale ( $\alpha_H = \alpha_s m_t$ ), shown as orange dashes, reproduces the full NLO result, represented by red crosses, as it contains the dominant terms close to threshold. On the other hand, we face the

problem that the resummed prediction keeps growing arbitrarily with  $\sqrt{s}$ , which is an artifact of the assumption that the computation is performed close to threshold and is seen by the rise of the green curve in Fig. 2. This is cured by multiplying the relevant scales with a switch-off function that smoothly approaches zero as one moves away from threshold. Combining these concepts gives a nice physical prediction in form of the blue dots. Note that while we have concentrated on the inclusive cross section here, the implementation in `WHIZARD` will eventually allow for the first time for arbitrary differential distributions with NLO+NLL precision together with their uncertainties based on scale variation.

#### 4. Acknowledgements

We want to thank Jonas Lindert for many useful discussions and especially the fast `OpenLoops` support. We also thank Tomáš Ježo for his advice about the resonance-aware FKS subtraction. JRR wants to thank the ACAT 2016 organizers for the beautiful venue in Valparaíso and a fantastic conference in Chile.

#### References

- [1] W. Kilian, T. Ohl, and J. Reuter. *EPJC* 71.9 (2011), p. 1742. arXiv:0708.4233.
- [2] M. Moretti, T. Ohl, and J. Reuter. *IKDA-2001-06, LC-TOOL-2001-040* (2001), p. 29. arXiv:0102195 [hep-ph].
- [3] T. Ohl. *CPC* 120.1 (1999), pp. 13–19. arXiv:9806432 [hep-ph].
- [4] T. Ohl. *CPC* 101.3 (1997), pp. 269–288. arXiv:9607454 [hep-ph].
- [5] W. Kilian, T. Ohl, J. Reuter, and C. Speckner. *JHEP* 2012.10 (2012), p. 22. arXiv:1206.3700.
- [6] W. Kilian, J. Reuter, S. Schmidt, and D. Wiesler. *JHEP* 2012.4 (2012), p. 13. arXiv:1112.1039.
- [7] T. Sjöstrand, S. Mrenna, and P. Skands. *JHEP* 2006.05 (2006), pp. 026–026. arXiv:0603175 [hep-ph].
- [8] T. Sjöstrand, S. Ask, J. R. Christiansen, et al. *CPC* 191 (2015), pp. 159–177. arXiv:1410.3012.
- [9] M. Bähr, S. Gieseke, M. A. Gigg, et al. *EPJC* 58.4 (2008), pp. 639–707. arXiv:0803.0883.
- [10] W. Kilian, D. Rainwater, and J. Reuter. *Physical Review D* 71.1 (2005), p. 015008. arXiv:0411213 [hep-ph].
- [11] K. Hagiwara, W. Kilian, F. Krauss, et al. *Physical Review D* 73.5 (2006), p. 055005. arXiv:0512260 [hep-ph].
- [12] M. Beyer, W. Kilian, P. Krstonošić, et al. *EPJC* 48.2 (2006), pp. 353–388. arXiv:0604048 [hep-ph].
- [13] A. Alboteanu, W. Kilian, and J. Reuter. *JHEP* 2008.11 (2008), pp. 010–010. arXiv:0806.4145.
- [14] J. Kalinowski, W. Kilian, J. Reuter, T. Robens, and K. Rolbiecki. *JHEP* 2008.10 (2008), pp. 090–090. arXiv:0809.3997.
- [15] W. Kilian, M. Sekulla, T. Ohl, and J. Reuter. *Physical Review D* 91.9 (2015), p. 096007. arXiv:1408.6207.
- [16] W. Kilian, T. Ohl, J. Reuter, and M. Sekulla (2015). arXiv:1511.00022.
- [17] P. Nason. *JHEP* 2004.11 (2004), pp. 040–040. arXiv:0409146 [hep-ph].
- [18] S. Frixione, P. Nason, and C. Oleari. *JHEP* 2007.11 (2007), p. 70. arXiv:0709.2092.
- [19] H. Baer, T. Barklow, K. Fujii, et al. *ILC-REPORT-2013* (2013). arXiv:1306.6352.

- [20] W. Kilian, J. Reuter, and T. Robens. *EPJC* 48.2 (2006), pp. 389–400. arXiv:0607127 [hep-ph].
- [21] J. Kalinowski, W. Kilian, J. Reuter, T. Robens, and K. Rolbiecki. *Acta Phys.Polon.* B39 (2008), pp. 1705–1714. arXiv:0803.4161.
- [22] T. Binoth, N. Greiner, A. Guffanti, et al. *Physics Letters B* 685.4-5 (2010), pp. 293–296. arXiv:0910.4379.
- [23] N. Greiner, A. Guffanti, T. Reiter, and J. Reuter. *Physical review letters* 107.10 (2011), p. 102002. arXiv:1105.3624.
- [24] S. Catani and M. Seymour. *Nuclear Physics B* 485.1-2 (1997), pp. 291–419. arXiv:9605323 [hep-ph].
- [25] R. Frederix, S. Frixione, F. Maltoni, and T. Stelzer. *JHEP* 2009.10 (2009), pp. 003–003. arXiv:0908.4272.
- [26] G. Cullen, N. Greiner, G. Heinrich, et al. *EPJC* 72.3 (2012), p. 1889. arXiv:1111.2034.
- [27] F Cascioli, P. Maierhöfer, and S Pozzorini. *Physical review letters* 108.11 (2012), pp. 1–5. arXiv:1111.5206.
- [28] S. Alioli, S. Badger, J. Bellm, et al. *CPC* 185.2 (2014), pp. 560–571. arXiv:1308.3462.
- [29] C. Weiss, B. C. Nejad, W. Kilian, and J. Reuter. *PoS(EPS-HEP2015)* (2015), p. 9. arXiv:1510.02666.
- [30] T. Ježo and P. Nason. *JHEP* 2015.12 (2015), pp. 1–47. arXiv:1509.09071.
- [31] M. Cacciari, G. P. Salam, and G. Soyez. *EPJC* 72.3 (2012), p. 1896. arXiv:1111.6097.
- [32] B. C. Nejad, W. Kilian, J. Reuter, and C. Weiss. *PoS(EPS-HEP2015)* (2015), p. 7. arXiv:1510.02739.
- [33] M. E. Luke, A. V. Manohar, and I. Z. Rothstein. *Physical Review D* 61.7 (2000), p. 074025. arXiv:9910209 [hep-ph].
- [34] A. Pineda. *Physical Review D* 66.5 (2002), p. 054022. arXiv:0110216 [hep-ph].
- [35] A. H. Hoang and P. Ruiz-Femenía. *Physical Review D* 74.11 (2006), p. 114016. arXiv:0609151 [hep-ph].
- [36] A. H. Hoang, C. J. Reiber, and P. Ruiz-Femenía. *Physical Review D* 82.1 (2010), p. 014005. arXiv:1002.3223.
- [37] A. H. Hoang and M. Stahlhofen. *JHEP* 2011.6 (2011), p. 88. arXiv:1102.0269.
- [38] A. H. Hoang and M. Stahlhofen. *JHEP* 2014.5 (2014), p. 121. arXiv:1309.6323.
- [39] A. H. Hoang and T. Teubner. *Physical Review D* 60.11 (1999), p. 114027. arXiv:9904468 [hep-ph].
- [40] F. Bach and M. Stahlhofen (2014). arXiv:1411.7318.